

## Controlling the Nusselt Number in a TiO<sub>2</sub>/R134a Nano-refrigerant System

Khaled M.K. Pasha

Associate professor of Mechanical Power, Faculty of Engineering, Modern University, Cairo, Egypt

Corresponding Author Email: [khmki1@yahoo.com](mailto:khmki1@yahoo.com)

<https://doi.org/10.18280/ijht.370122>

**Received:** 30 September 2018

**Accepted:** 20 January 2019

**Keywords:**

*refrigeration, nano-, evaporator, heat flux, reynolds*

### ABSTRACT

Experimental runs were performed to investigate the variation of the evaporator Nusselt number with the Reynolds number, the heat flux and the nano-Particles concentration in a refrigeration system. The used refrigerant is TiO<sub>2</sub>/R134a nano-fluid at different values of nano-particle concentration. Next, the refrigeration system was modified with an auxiliary evaporator and a control unit which will store the experimental results. These results will be used as a guide to distribute the mass and heat fluxes between the two evaporators. So, it is possible to control the Nusselt number and accordingly, to achieve a predetermined variation of the cooling behavior in more than one evaporator. The experimental results showed that, for all studied cases, the Nusselt number increased with the Reynolds number and the heat flux. The Nusselt number also increased with the Nano-Particle concentration up to the value of 0.5, and beyond this value, its enhancement started to deteriorate. When increasing the Reynolds Number by about 98 % the Nusselt number could be enhanced by about 67 %. Two correlations were suggested to fit the data of the Nusselt number, the heat flux, and the nano-particles concentration. This research work is a step towards the control of many cooling loads using one compressor.

## 1. INTRODUCTION

### 1.1 Theoretical investigation

For all refrigeration and HVAC systems, the heat transfer in the evaporator is an essential factor that assists the system performance and efficiency. One of the widely used refrigerants is R134a because it is widely accepted alternative refrigerant due to its low ozone depletion potential. It has a strong chemical polarity that allows the traditional mineral oil, mixed with it to be used as a lubricant and it is available and relatively less expensive. Many Researchers showed that, when using TiO<sub>2</sub>/ R134a nano-refrigerant in a refrigeration system, a considerable heat transfer enhancement occurs in its evaporator and, its compressors power is reduced too. Patil et al. [1] reviewed the thermal properties of nano-refrigerants and the energy consumption of its refrigerant systems. They reported that, when using 0.1 % mass fraction of TiO<sub>2</sub> with POE, the energy consumption is reduced by 26.1 % of that in the case without TiO<sub>2</sub>. The freezing rate is slightly higher with the system with TiO<sub>2</sub> as compared to the case of POE oil without TiO<sub>2</sub>. For many nano-particles that are dispersed in r134a, the effective thermal conductivity decreases with the particle size. But, it is still higher than the corresponding values of the cases where no nano-particles are added. The thermophysical and the heat transfer characteristics of TiO<sub>2</sub>-R134a nano-refrigerants were investigated during the boiling process by Sanukrishna et al. [2] They observed that the presence of TiO<sub>2</sub> in a refrigerant can enhance the thermophysical properties and accordingly, the heat transfer coefficient could increase by 30.2 % when the particle concentration is 1.5 %. Yang and Hu [3] summarized the recent researches of the application of TiO<sub>2</sub>

nano-fluids. They concluded that, the thermal conductivity of nano-refrigerant increases with the volume fraction of TiO<sub>2</sub>. For 5 % volume fraction of TiO<sub>2</sub> and temperature of 343 K, the enhancement in the thermal conductivity may reach the value of 30 %. The thermal conductivity also increases with temperature. At temperature 60 °C, the nano-refrigerant, which includes 4 % TiO<sub>2</sub> nano-particles of average size 26 nm, attained 19 % enhancement in the thermal conductivity. Also, when using R134a and mineral oil with TiO<sub>2</sub> nano-particles of size 50 nm and at concentration 10 g/L, the energy consumption of the system decreased by 7.43 %. In addition, using R134a and mineral oil with TiO<sub>2</sub> nano-particles of size 50 nm and at concentration 0.1 % wt., the energy consumption of the system decreased by 26.1 %. Alawi et al. [4] investigated TiO<sub>2</sub> nano-particles at very low concentrations with different refrigerants. They reported that the thermal conductivity is strongly temperature-dependent than that in the case of conventional refrigerant. Modifications to the thermophysical properties are the primary mechanism that affects heat transfer performance during flow boiling of nano-fluids. Increasing the thermal conductivity enhances the heat transfer, but, increasing the viscosity and surface tension reduces the heat transfer in nucleate boiling-dominated flows. A secondary mechanism appears when nano-particles fill up the micro-cavities on the test surface. It is also responsible for the decreased heat transfer and is a strong function of particle number density Kolekar et al. [5]. For a refrigeration system, many factors affect its thermal performance and its compressor power saving. Ajuka et al. [6] investigated the effects of evaporator temperature on the power consumption, coefficients of performance, exergetic efficiency and efficiency defects in the compressor, condenser, capillary tube and evaporator of

the system. They used refrigerants R600a and LPG (R290/r600a: 50 %/ 50 %) at 0, 0.05, 0.15 and 0.3wt % concentrations of 15nm particle size of (TiO<sub>2</sub>) nano-lubricant, and (r134a). They concluded that, LPG + TiO<sub>2</sub> (0.15wt %) and R600a + TiO<sub>2</sub> (0.15wt %) had the best performances with an average of 27.6% and 14.3% higher coefficient of Performance, 34.6 % and 35.15% lower power consumption. TiO<sub>2</sub> nano-particles also increase the compatibility between the mineral oil and r134a, and the system that uses their mixture works safely with higher performance than that which uses r134a/POE alone. TiO<sub>2</sub> nano-particles can enhance the heat transfer of the refrigerator system and also strengthen the lubrication capability of mineral oil, Yong et al. [7]. Adding TiO<sub>2</sub> nano-particles at a concentration that ranges from 0.05 to 1 %, to R134 could enhance the heat transfer coefficient by a value of 50 % of that for the case pure fluid, Naas [8]. Using 0.1 % TiO<sub>2</sub>- mineral oil-R134a in a domestic Refrigerator has caused a maximum energy saving of (25 %), Javadi et al. [9]. The effect of 0.06 % TiO<sub>2</sub> resulted in better saving than that of 0.1 % Al<sub>2</sub>O<sub>3</sub>. This reflects the deterioration of performance with the increase of TiO<sub>2</sub> concentration and this result agrees with the conclusion of the present work. Subramani.N et al. [10] investigated the performance parameters of a vapor compression system with pure SUNISO 3GS oil and with different nano-lubricants. They reported that the freezing capacity was higher for TiO<sub>2</sub> nano-lubricant compared with other studied cases. For the case of TiO<sub>2</sub>, they could achieve a reduction of 15.4 % in the compressor power. Padmanabhan and Palanisamy, [11] added 0.1 g of (TiO<sub>2</sub>) to each liter of Mineral oil, MO, that is mixed with (r134a), R436A and R436B. They reported that the total irreversibility (529, 588 and 570 W) at different process was better than the cases, where no TiO<sub>2</sub> is used. Adelekana et al. [12] investigated varied mass charges of Liquefied Petroleum Gas (40 g, 50 g, 60 g and 70 g) with different (TiO<sub>2</sub>) nano-particle/ mineral oil concentrations (0.2 g/L, 0.4 g/L and 0.6 g/L nano-lubricants) in a R134a in a domestic refrigerator. They achieved a reduced compressor power input of about 21 W with the 70 g of LPG with either of 0.2 g/L or 0.4 g/L nano-lubricants. With 70 g of LPG using 0.6 g/L concentration of nano-lubricant, they could attain a cooling capacity index of 65 W. The highest COP of 2.8 was obtained with 40 g charge of LPG using 0.4 g/L concentration of nano-lubricant. Increasing the concentration of nano-particles (TiO<sub>2</sub>) in refrigerant results in an increase in the performances of the refrigeration system due to the decrease in the compressor work and the enhancement in the heat transfer rate. But for a system that works at high pressure in hot and dry climate condition, the performances of the condenser decreases. So, it is recommended to couple the vapor compression refrigeration system with an evaporative cooling pad. Dhamneya et al. [13] used this technique and reported a maximum increase in C.O.P. of about 51 %. Shengshan Bi et al. [14] experimentally investigated the nano-refrigerant TiO<sub>2</sub>-R600a in a domestic refrigerator using energy consumption test and freeze capacity test. They achieved an energy saving of 9.6% when they used TiO<sub>2</sub> at a concentration of 0.5 g per each liter of r600a. They also obtained a better refrigerator performance than that of the pure R600 case. The idea of mixing more than nano-particle was investigated by Raghavulu et al. [15]. Nano-refrigerants Al<sub>2</sub>O<sub>3</sub>-Ethylene glycol oil and TiO<sub>2</sub>-Ethylene glycol oil were added to r134a. They reported that,

when adding Al<sub>2</sub>O<sub>3</sub> to R-134a, the COP of vapor compression refrigeration system improved by 12.08 % of that which does not use nano-particle. For the domestic refrigerator that uses LPG refrigerant with (TiO<sub>2</sub>) nano-particles dispersed in a mineral oil lubricant, the cooling capacity and COP of could be improved by 18.74–32.72 and 10.15–61.49 %, respectively. Furthermore, compressor power consumption and pressure ratio were decreased by about 3.20–18.1 and 2.33–8.45 %, respectively, Gill et al. [16]. TiO<sub>2</sub> in the form of nano-particles may enhance the heat transfer coefficient. Also, TiO<sub>2</sub> in the form of nano-layer can enhance the heat transfer coefficient. Ray et al. [17] investigated the pool boiling of R134a on flat copper surfaces that are fabricated with titanium dioxide (TiO<sub>2</sub>) thin film (TF) coating of thickness 100 nm and 200 nm. They reported that, with the 200 nm coating thickness, the heat transfer coefficient achieved the maximum enhancement over that of the case with uncoated copper surface. This heat transfer coefficient enhancement is due to augmented roughness and increment of dynamic nucleation site density. Ray et al. [18] also investigated the pool boiling at 10 °C of R134a on flat copper surfaces that are coated with thin film of TiO<sub>2</sub> nano-particles, and the film thicknesses are 100 nm, 200 nm, and 300 nm. They achieved a maximum of 87.5 % augmentation in the boiling heat transfer by the higher thickness of TiO<sub>2</sub> coated surface than the bare copper surface. They interpreted the augmentation of heat transfer coefficient by the increase in micro/nano-porosity, active nucleation site density and surface area of the heating surface. The refrigerant R134 was tested with different nano-particles; Coumaressin and Palaniradja [19] investigated the refrigerant R134a with CuO nano-particle in a counterflow heat exchanger evaporator which is similar to that used in the present work. They evaluated the heat transfer coefficients for heat flux that ranged from 10 to 40 kW/m<sup>2</sup> and used nano-particle concentrations that ranged from 0.05 to 1% and particle size from 10 to 70 nm. They reported that the heat transfer enhancement increased with the nano-particle concentration until a concentration of 0.55 %, and beyond this value, the enhancement rate started to deteriorate. This observation is similar to what was observed in the results of the present work. The effect of pressure on the heat transfer process attracted some researchers to investigate it. Cieśliński and Kaczmarczyk investigated the heat transfer coefficient during the pool boiling processes in a horizontal tube [20]. They tested two nano-fluids; water-Al<sub>2</sub>O<sub>3</sub> and water-Cu at the concentration of 0.01 %, 0.1 %, and 1 % by weight. They established that increasing the operating pressure results in an enhancement in the heat transfer coefficient. Finally, not all refrigeration systems show enhancements in the heat transfer coefficient when using nano-refrigerants, but in some investigated cases, the performance deteriorates, and this agrees with the results of the present work. Kolekar et al. [5] obtained stable nano-fluids by mixing R134a with dispersions of surface-treated nano-particles TiO<sub>2</sub> in polyol ester (POE) oil (RL22H and RL68H). They investigated the flow boiling over a range of mass flux from 100 to 1000 kg/m<sup>2</sup> s, with a heat flux from 5 to 25 kw/m<sup>2</sup>, and vapor quality up to 1. They reported that the heat transfer coefficients decreased by 28 % TiO<sub>2</sub>/CO<sub>2</sub> nano-fluids.

## 1.2 Objectives of the present work

In the present work, it is intended to accomplish two tasks;

1- To investigate experimentally the variation of the 'evaporator' Nusselt number with Reynolds number, the heat flux, and the Nano-Particles concentration for a refrigeration system that uses the nano-refrigerant (TiO<sub>2</sub>- RL 32 POE) /r134a.

2- To modify the system with an auxiliary evaporator and a control unit that will store the experimental data and use them in controlling the heat and mass fluxes, in order to achieve a predetermined heat transfer behavior.

Table 1 illustrates the different studied cases.

**Table 1.** TiO<sub>2</sub> mass concentration, heat flux mass flux and Reynolds number for the investigated cases

TiO <sub>2</sub> Concentration, %	Heat Flux, q, (Kw m <sup>2</sup> )	Reynolds number, Re
0.05	33.17	4805
0.05	44.25	6387
0.05	56.53	8039
0.05	67.5	9597
0.3	33.4	4810
0.3	44.8	6413
0.3	57.14	8054
0.3	68.29	9608
0.5	33.4	4815
0.5	44.8	6400
0.5	57.14	8047
0.5	68.29	9604
1	33.2	4830
1	44.38	6421
1	56.74	8060
1	67.83	9611

### 1.3 Paper outlines

The rest of this paper will include the experimental preparations and the procedure followed in each experimental run. Also, the results will be illustrated with comments and interpretation when possible. Following is a conclusion of the whole work and results is set. The used terms and

abbreviations are sorted in a list. More relevant details are mentioned in the appendices. Finally, the references are sorted alphabetically.

## 2. EXPERIMENTAL SETUP

### 2.1 The primary test rig

The primary test rig, Figure 1, was implemented according to Naas [8] and it consists mainly of the following components;

The Compressor is of type TECUMSEH sealed hermetic reciprocating type of one HP, 220 volts, and 50 Hz.

The Condenser is a heat exchanger which consists of two concentric copper tubes, and have a length of 1700 mm. The inner tube, where the refrigerant flows, has an outer diameter of 9.52 mm, ( 3/8 inch), and the inner diameter of 7.72 mm, (2.47/8 inch). The outer tube, where the water flows, has an outer diameter of 19.05 mm, ( 3/4 inch), and the inner diameter of 17 mm, (0.68 inches).

The Main Evaporator, Figure 2, is a heat exchanger which consists of two concentric copper tubes and has a length of 1260 mm. The outer tube, where the water flows, has an outer diameter of 19 mm, and the inner diameter of 17 mm. The outer tube is divided into 10 segments, each segment has an independent inlet and exit terminals. This structure promotes the turbulent mixing activities of the flowing water and accordingly,

enhances the evaporation of the flowing refrigerant. The inner tube, where the refrigerant flows, has an outer diameter of 9.5 mm and an inner diameter of 7.5 mm. The refrigerant mass flow rate and accordingly the Reynolds number could be varied by a valve whose opening is controlled by a stepper motor.

The Pump is QB Series Peripheral 0.25 hp water pump, and it is interfaced to the controller which maintains the water discharge at a fixed rate of 0.74 kg/s.

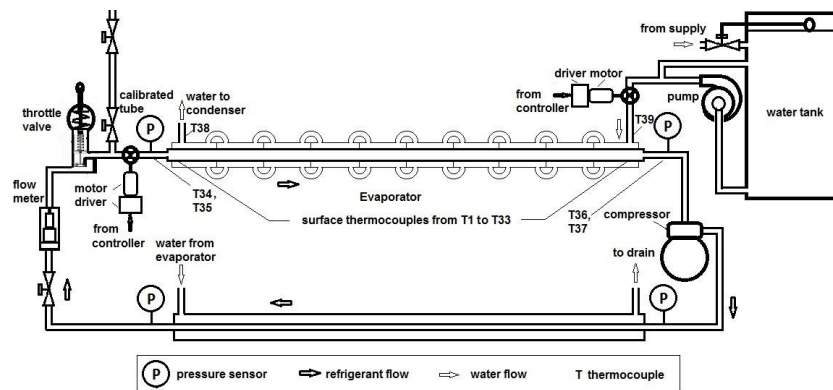


**Figure 1.** The primary test rig

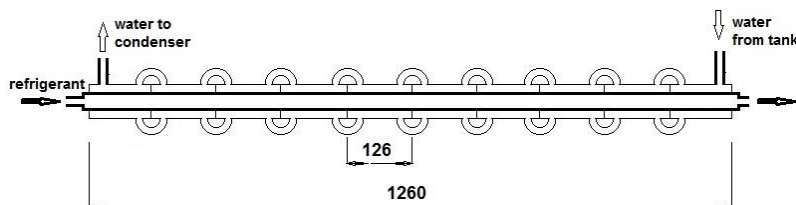


**Figure 2.** The main evaporator

## 2.2 The measuring and control devices

- PIC32MX3/4 microcontroller
- thirty-three thermocouples, T1 to T33, are distributed on eleven positions on the surface and another two pairs of thermocouples, T34 to T37, are placed in the refrigerant flow passage, before and after the evaporator. An additional two thermocouples, T38 and T39, are placed in the *water* passage before and after the evaporator to measure the change in water temperature. All these thermocouples are of type (T) and well calibrated before usage.
- three TCA9546-i2C Mux and six i2c-MCP9600 thermocouple chips connect the thermocouples to the controller. Four pressure sensors are distributed as follows; two of them are placed before and after the evaporator, and each of them has a maximum reading of 10 bars, and the other two sensors are placed before and after the condenser, each of them has a maximum reading of 32 bars.
- Two control valves that are driven by stepper motors with their drivers. Each valve is first calibrated to determine the relation between the motor turns and the corresponding flow rate. Then, they are installed in the passages of the water and refrigerant before the evaporator.
- The refrigerant flow rate is measured using an Omega F1-2100A flow meter, (5), which measures values from 0.2 to 1.9 liter/min, with an accuracy of 0.05 liter/min.
- The high and low cycle pressures are adjusted using an adjustable throttle valve (3), Dofun-TVD-A that maintains the evaporator pressure at 4 bar.
- The water flow rate is measured using a DZ-4002 flow meter, which measures values from 1.8 to 18 liter min<sup>-1</sup>.
- The masses are weighed by an electronic balance RUIIM D-8001 with Readability 0.01 gm.

The signals from thermocouples, pressure sensors, and the flow rate sensors are fed from the microcontroller to a PC program, which calculates the corresponding heat flux, the Reynolds number, and the Nusselt number, Eq. (1-13).

## 2.3 The experimental procedure

Before beginning, the following procedure is followed;

- operating the pump at max power for 10 minutes to check the water passages
- The fabricated experimental setup is filled with N2 gas at a pressure of 7 bar and this pressure is maintained for 45 minutes for the purpose of leakages check, (5).
- reviewing the connections of the control components and measuring devices
- The cycle is evacuated using a vacuum sealed vessel.

In every experiment, the following steps were followed;

- 1) weighing the calculated mass of Nano-Particles *s*, using digital electronic balance, and adding them carefully to the corresponding weight of Emcarate RL 32 POE oil, according to Table 2.
- 2) The mixture is placed on the ultrasonic vibrator for 3 hours to ensure uniform dispersion of Nano-Particles *s*, [5].
- 3) The mixture is further kept vibrating for an additional half an hour, on an ultrasonic homogenizer to fully separate the Nano-Particles and to prevent any clustering of particles in the mixture, and to obtain proper homogenization, and then added to the cycle.
- 4) Operating the compressor and after 10 minutes, the controller starts to feed the computer with the signals of temperature before and after the evaporator for the water and

refrigerant, and the signals from the flow meters of both liquids. The program calculates the corresponding average surface and refrigerant temperatures, equation (1-3). It then uses equations (4-8) in order to calculate the different Nano-Fluid properties. From the initial refrigerant flow rate and applying simple energy conservation, an *initial* value for the water flow rate is obtained.

5) The controller adjusts the water valve opening according to this value. Keeping receiving newer signals from these sensors, the program *recalculates newer* water flow rates, and according to a PID technique, the water rate keeps modifying until the difference between the newer and older values is within 2%.

6) After achieving a steady state, the program uses the input data to calculate the corresponding Nusselt number.

**Table 2.** Preparing the Nano-Lubricant

Nano-Particles concentration, <i>z</i>	<i>Z</i> = 0.05 %	<i>Z</i> = 0.3 %	<i>Z</i> = 0.5 %	<i>Z</i> = 1 %
Lubricant, (gram)	3	18	30	60
R134a, (gram)	596.7	580.2	567	534
Nano-, (gram)	0.3	1.8	3	6

$$T_{s,av} = \frac{\sum_{i=1}^{33} T_{si}}{33} \quad (1)$$

$$T_{si} = T_{top} + T_{bottom} + T_{side} \quad (2)$$

$$T_{nf,av} = (T_{in} + T_{out})_{nf} / 2 \quad (3)$$

According to Nass [8], the volume fraction, the density and the specific heat are calculated as follows;

$$100 \phi = \frac{z\rho_f}{\rho_{np}(1-z) + z\rho_f} \quad (4)$$

$$\rho_{nf} = \phi \rho_{np} + (1-\phi)\rho_f \quad (5)$$

$$Cp_{nf} = \frac{\phi(\rho Cp)_{np} + (1-\phi)(\rho Cp)_f}{\rho_{nf}} \quad (6)$$

And according to Subramani [10];

$$\mu_{nf} = \mu_f [1/(1-\phi)^{2.5}] \quad (7)$$

And according to sanukrishna [2];

$$\frac{k_{nf}}{k_f} = \frac{k_p + 2k_f - 2\phi(k_f - k_p)}{k_p + 2k_f - \phi(k_f - k_p)} \quad (8)$$

$$m^* = (V \rho^*)_{nf} \quad (9)$$

$$Re = \frac{4 m_{nf}^*}{10^3 \pi d_i L \mu_f} \quad (10)$$

The program estimates an *initial water* flow rate,  $m_w^*$  from an intended heat flux according to;

$$q A_s = m_w C_w (T_{iw} - T_{ow}) \quad (11)$$

$$h = \frac{[m C_p (T_o - T_i)]_{nf}}{\pi d_i L (T_{s,av} - T_{nf,av})} \quad (12)$$

$$Nu = \frac{10^3 h d_i}{k_{nf}} \quad (13)$$

The cycle coefficient of performance;

$$C.O.P = \frac{Cp(T_o - T_i)_{nf,e}}{Cp(T_o - T_i)_{nf,c}} \quad (14)$$

The worst *relative* errors that may occur when measuring the above quantities are illustrated in Appendix A.

Some of the experimental results of the heat transfer coefficient of the used nano-refrigerant, TiO<sub>2</sub>/R134a are illustrated in figure 3. The figure also illustrates the results of Naas, [8], Alawi, et al, [4] and Sanukrishna et al. [2] for the same nano- refrigerant but, at different pressure values. It is obvious that all the cases have the same trend of variation but, the results of the present work are more close to those of Naas because both cases have the same conditions of the applied pressure and particle concentration and. As mentioned above, increasing the operating pressure results in an enhancement in the heat transfer coefficient, Cieřliński and Kaczmarczyk [20]. The results of Alawi were obtained under lower pressure than what was applied in the present work. Whereas, the applied pressure in the case of Sanukrishna was higher than that of the present work.

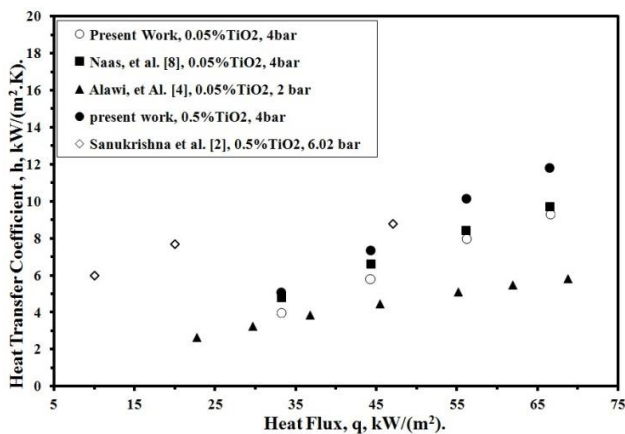


**Figure 3.** Data from the present work and from Alawi [4], Naas [8] and Sanukrishna [2] at different pressure conditions

### 3. RESULTS AND DISCUSSION

#### 3.1 The experimental results

These experiments are executed to investigate the variation of the Nusselt number, with the heat flux and the Reynolds number. Figure 4 illustrates the variation of Nusselt number with the heat flux and Figure 5 illustrates the variation of Nusselt number with the Reynolds number. First observation in Figure 5 is that the *position* of each data point of the heat

flux and the Reynolds number differs slightly with the increase of particles concentration. That is because increasing the concentration leads to an increase in the mass flow rate and accordingly, the Reynolds number slightly increases for the same flow rate. The thermal conductivity and the thermal transport capabilities increase with the concentration too, and this affects the heat flux for the same flow rate. For all studied cases, the Nusselt number increases with the particles concentration until  $z=0.5\%$  and beyond this value, it starts to decrease again. That may be because, when the particles concentration increases, the mass flow rate increases, equation 4, 5 and 9, and accordingly the mixture thermal conductivity and capacity of carrying more heat increase too. In such conditions, the possibility of increasing the bulk fluid temperature increases. So, the difference in temperature between the fluid and the surface decreases, which helps the heat transfer coefficient to increase, Eq. 12.

The thermal conductivity also increases with the concentration, equation 8, at a lower rate than that of the heat transfer coefficient, and this helps the Nusselt number to increase too equation 13. But, increasing the particles concentration may lead to narrower passages for the particles to move through the fluid and a reduction in the Nano-Particles mobility under the thermophoretic forces and accordingly, its convective heat transfer decreases. So, increasing the Nano-Particle concentration produces two opposing factors; one promotes for the increase in Nusselt number, which is dominant for a Nano-Particles concentration less than 0.5 %, and the other decays it, which starts to be dominant for  $z>0.5\%$ .

In Figure 4, the Nusselt number increases with the heat flux, for all values of concentration. That may be because, increasing the heat flux, promotes for a higher refrigerant superheat, which in turn increases the average refrigerant temperature and reduces the temperature difference between the refrigerant and the surface. This leads to an increase in heat transfer coefficient, but a small increase in the refrigerant thermal conductivity, which depends mainly on the temperature, and the majority of the process in the evaporator is a phase change, and accordingly, the Nusselt number increases.

From Figure 5, the Nusselt number increases with the Reynolds number, for all values of concentration. That may be because, increasing the fluid flow rate promotes for a higher possibility of exchanging more thermal energy with the tube surface, which leads to a decrease in the average temperature difference between the surface and fluid, meanwhile, the heat transfer is increased. That may result in a higher heat transfer coefficient with a little change in the thermal conductivity. Consequently, the ratio between the heat transfer and the thermal conductivity increases and accordingly, the Nusselt number increases. The maximum percentage of enhancement in the Nusselt number was 112 % and occurred when increasing the Reynolds number by about 99.7 % of its lowest value.

Figure 6 illustrates the variation of C.O.P with heat transfer coefficient. For all Nano-Particle concentration, the C.O.P varies slightly with the Nusselt number, which reflects that, the ratio of the heat transfer rate and the compressor power increase *slightly* with the Nusselt number. In other words, the compressor power and the cycle losses are *almost* proportional to the refrigerant mass flow rate. But the relation between the heat transfer rate and the refrigerant mass flow rate is not linear. For the same Nusselt number, the rate of

heat transfer increased with the particle concentration with a little increase in the compressor power, so, the COP increased. And again the concentration of Nano-Particles *considerably* affects the heat transfer, and *slightly* increases the compressor power, which leads to an increasing COP whenever the particle concentration is lower than 0.5 %. This behavior is reversed when the particle concentration exceeds 0.5 %, where the Nusselt number starts to decrease for the reasons mentioned above.

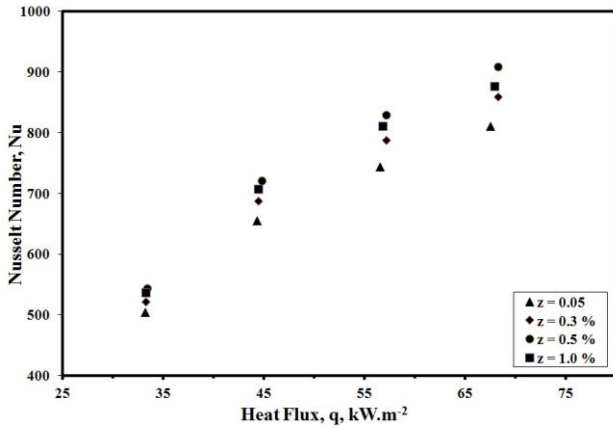


Figure 4. Variation of Nusselt number with the heat flux

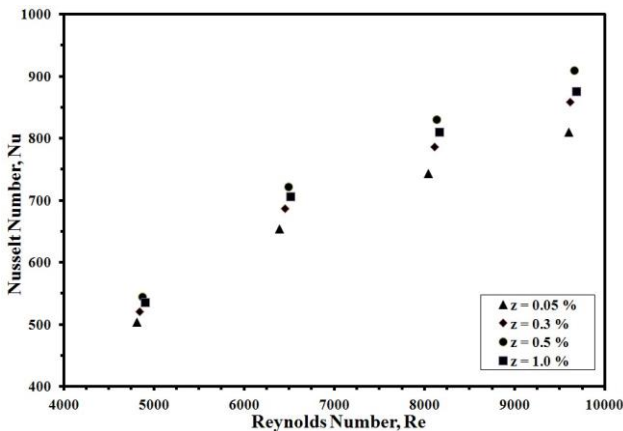


Figure 5. Variation of Nusselt number the Reynolds number

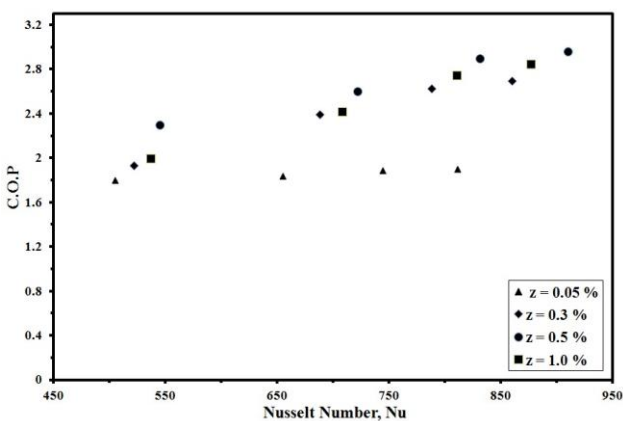


Figure 6. Variation of C.O.P with the Nusselt number for different nano-particle concentrations

After trying different formulas to fit the experimental data, one of them could fit the data with minimum deviation,

equations 15. This equation relates the Nusselt number to the Nano-Particle concentration, the Reynolds number, and the heat flux. The worst deviation of the calculated Nusselt values from these measured by the correlation was about 5%. Appendix B illustrates samples of the calculated and measured data.

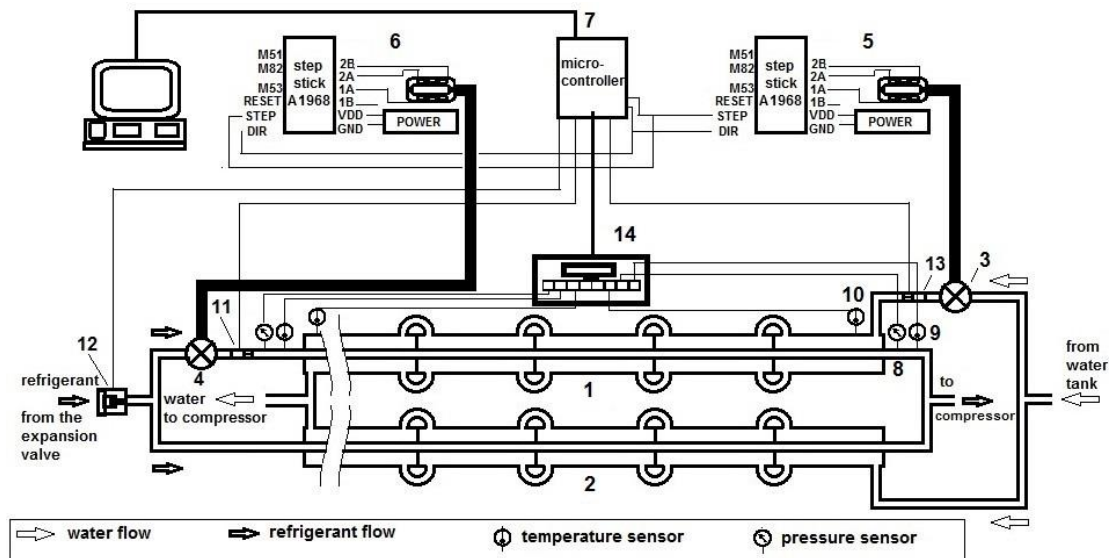
$$Nu = 0.18 z^{0.02} \times Re^{1.1} \times q^{-0.36} \quad (15)$$

### 3.2 Controlling the Nusselt number

In these experiments, it is required to **vary** the Nusselt number of the main evaporator with time according to a predetermined behavior. Figure 7 illustrates the preparation of the control experiment. The figure illustrates a secondary evaporator, which is similar to the main evaporator, is installed to share the water and refrigerant flow rates. The two controlled valves are installed in the entrance to the main evaporator; one of them controls the refrigerant flow rate and the other controls the hot water flow rate. The experimental data of the heat flux, Reynolds number and the Nusselt number that is extracted from the experiments, whose Nano-Particles concentration is 0.5 % are fed to the program. According to these data, the controller produces the required variation in the heat flux, the Reynolds number and accordingly, the required Nusselt number. To execute this type of experiments, the preparations and steps from (1 to 5) that are mentioned in 2.2 are followed and then;

- (1) The controller should adjust the system actuators to produce a Reynolds number of about 4866 and a heat flux of 33.4 kW/m<sup>2</sup> which correspond to a Nusselt number of about 575. Then, it should maintain the Nusselt number at this value for 60 minutes.
- (2) Next, the controller should adjust the Nusselt Number value to be 720 approximately which corresponds to a Reynolds number of 6488 and a heat flux of 44.8 kW/m<sup>2</sup>. Then, it should maintain the Nusselt number at this value for 80 minutes.
- (3) Finally, the controller should adjust the Nusselt Number value to be 910 approximately which corresponds to a Reynolds number of 9655 and a heat flux of 68.3 kW/m<sup>2</sup>. Then, it should maintain the Nusselt number at this value for 100 minutes.

During the operation, the data of the Nusselt number are monitored every 10 minutes. Figure 8 illustrates the variation of the Nusselt number with time. It is observed that, the Nusselt number value during each of the three time intervals is not stable, that is because, at the beginning of each interval, the controller changes the heat flux and Reynolds number according to the values that are mentioned above, and a PID scheme helps these quantities to approach almost a steady value, and consequently, a required Nusselt value. This scheme keeps guarding the achieved values to maintain them from the random change in the ambient conditions and unpredicted losses. Also, the limited speed, memories, and storage capacity of the used controller did not ensure the proper speed of response to the feedback signals. That is beside the fluctuating nature of the variation in the ambient conditions during the day hours, which is an inherent characteristic of the weather in the city, where these experiments are performed. These random variations may lead to unpredicted losses in the hot water side as well as the refrigerant side of the refrigeration.



- 1- Main evaporator
- 2 secondary evaporator
- 3- water control valve
- 4- refrigerant control valve
- 5- stepper motor+driver, (water valve)
- 6- stepper motor+driver, (refrigerant valve)
- 7- microcontroller
- 8- refrigerant pressure sensor
- 9- refrigerant temperature sensor
- 10- water temperature sensor
- 11- main evaporator refrigerant flow sensor
- 12- total refrigerant flow sensor
- 13- main evaporator water flow sensor
- 14- thermocouple interface

Figure 7. The control unit installation

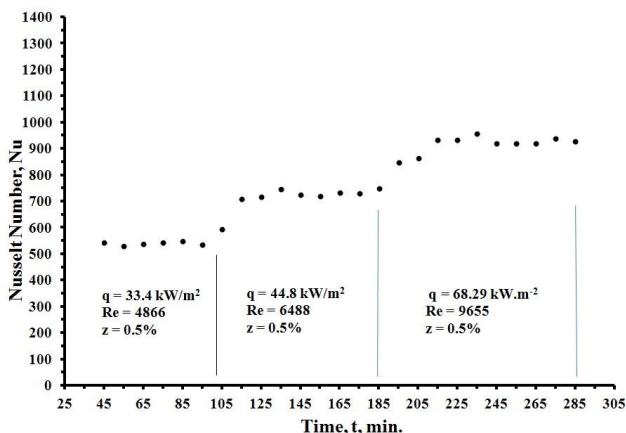


Figure 8. The control experiment

#### 4. CONCLUSION

An experimental investigation was executed to study the variation of the 'evaporator' Nusselt number with the heat flux, Reynolds number, at four values of Nano-Particles concentration, (z), in a vapor compression refrigeration system, whose refrigerant is a TiO<sub>2</sub>/R134a Nano-Fluid. The Nusselt Number increased with the Reynolds number and heat flux in all studied cases. It also increased with the Nano-Particle concentration to the value of 0.5% and beyond this value, a deterioration appeared in its enhancement. The percentage of increase in the Nusselt number achieved a maximum value of 67% when increasing the Reynolds number by about 98% of its lowest value.

Next, the test rig was modified with a secondary evaporator and a control unit which will store the experimental data of the heat flux and the Reynolds number along with the nano-particle concentrations. These data guided the controller to follow a predetermined variation in the Nusselt number and accordingly, to control the cooling behavior.

The experimental results suggested a correlation which expressed the variation of the Nusselt number with both; the Reynolds number and the heat flux at different values of the Nano-Particle concentrations. The present work may be considered as a **step to future** work, in which, a Nano-Refrigerant system contains a single compressor, that supplies many evaporators situated in different regions in the installation.

#### REFERENCES

- [1] Patil MS, Kim SC, Seo JH, Lee MY. (2016). Review of the thermo-physical properties and performance characteristics of a refrigeration system using refrigerant-based nanofluids. *Energies* 9(1): 22. <https://doi.org/10.3390/en9010022>
- [2] Sanukrishna SS, Ajmal N, Prakash MJ. (2018). Thermophysical and heat transfer characteristics of R134aTiO<sub>2</sub> nanorefrigerant: A numerical investigation. *28th International Conference on Low Temperature Physics (LT28) IOP Publishing IOP Conf. Series: Journal of Physics: Conf. Series* 969(2018): 012015. <https://doi.org/10.1088/1742-6596/969/1/012015>

- [3] Yang L, Hu YH. (2017). Toward TiO<sub>2</sub> Nanofluids—Part 2: Applications and Challenges 12: 446. <https://doi.org/10.1186/s11671-017-2185-7>
- [4] Alawi OA, Mohammed HA, Sidik NAC. (2014). A comprehensive review of fundamentals, preparation, and applications of nano-refrigerants. *International Communications in Heat and Mass Transfer* 54: 81-95. <https://doi.org/10.1016/j.icheatmasstransfer.2014.03.001>
- [5] Kolekar RD. (2014). An experimental study of the flow boiling of refrigerant-based nanofluids. Dissertation, Phd, The Graduate College of the University of Illinois At Urbana-Champaign.
- [6] Ajuka LO, Odunfa MK, Ohunakin OS, Oyewola MO. (2017). Energy and exergy analysis of vapour compression refrigeration system using selected eco-friendly hydrocarbon refrigerants enhanced with TiO<sub>2</sub>-nanoparticle. *International Journal of Engineering & Technology* 6(4): 91-97. <https://doi.org/10.14419/ijet.v6i4.7099>
- [7] Yong H, Bi SS, Shi L. (2006). Refrigerator with R134a/TiO<sub>2</sub> nanoparticle system, *Huagong Xuebao/ Journal of Chemical Industry and Engineering (China)* 57: 141-145.
- [8] Naas KSM. (2016). Heat transfer enhancement in vapor compression refrigeration system using nano-fluid with R-134a. Thesis, Benha University, Faculty of Engineering, Mechanical Engineering Department.
- [9] Javadi FS, Saidur R. (2016). Energetic, economic and environmental impacts of using nanorefrigerant in domestic refrigerators in Malaysia. *Energy Conversion and Management* 73: 335-339. <https://doi.org/10.1016/j.enconman.2013.05.013>
- [10] Subramani N, Mohan A, Prakash JM. (2013). Performance studies on a vapour compression refrigeration system using nano-lubricant. *International Journal of Innovative Research in Science, Engineering and Technology* 2(Special Issue 1). Proceedings of International Conference on Energy and Environment-2013 (ICEE 2013) On 12th to 14th December.
- [11] Padmanabhan VMV, Palanisamy S. (2012). The use of TiO<sub>2</sub> nanoparticles to reduce refrigerator ir-reversibility. *Energy Conversion and Management* 59: 122-132. <https://doi.org/10.1016/j.enconman.2012.03.002>
- [12] Adelekana DS, Ohunakina OS, Babarindea TO, Odunfaa MK, Leramo RO, Oyedepoa SO, Badejoa DC. (2017). Experimental performance of LPG refrigerant charges with varied concentration of TiO<sub>2</sub> nano-lubricants in a domestic refrigerator. *Case Studies in Thermal Engineering* 9: 55-61. <https://doi.org/10.1016/j.csite.2016.12.002>
- [13] Dhamneya AK, Rajput SPS, Singh A. (2018). Comparative performance analysis of ice plant test rig with TiO<sub>2</sub>-R134a nano refrigerant and evaporative cooled condenser. *Case Studies in Thermal Engineering* 11: 55-61. <https://doi.org/10.1016/j.csite.2017.12.004>
- [14] Bi SS, Guo K, Liu ZG, Wu JT. (2011). Performance of a domestic refrigerator using TiO<sub>2</sub>-R600a nano-refrigerant as working fluid. *Energy Conversion and Management* 52(1): 733-737. <https://doi.org/10.1016/j.enconman.2010.07.052>
- [15] Raghavalu KV, Reddy PS, Khan AR, Kumar DV, Prashanth T. (2016). Improvement of COP of vapor compression refrigeration system by using nano-refrigerants. *IJSRD || National Conference on Recent Trends & Innovations in Mechanical Engineering || April*, pp. 172-175.
- [16] Gill J, Singh J, Ohunakin OS, Adelekan DS. (2018). Energy analysis of a domestic refrigerator system with ANN using LPG/TiO<sub>2</sub>-lubricant as replacement for R134a. *Journal of Thermal Analysis and Calorimetry* 135(1): 1-14. <https://doi.org/10.1007/s10973-018-7327-3>.
- [17] Ray M, Deb S, Bhaumik S. (2017). Experimental investigation of nucleate pool boiling heat transfer of R134a on TiO<sub>2</sub> coated TF surface. *Materials Today: Proceedings* 4(9): 10002-10009. <https://doi.org/10.1016/j.matpr.2017.06.310>
- [18] Ray M, Bhaumik S. (2018). Nucleate pool boiling heat transfer of hydro-fluorocarbon refrigerant R134a on TiO<sub>2</sub> nanoparticle coated copper heating surfaces. *Heat Transfer Engineering*. <https://doi.org/10.1080/01457632.2018.1450333>
- [19] Coumaressin T, Palaniradja K. (2014). Performance analysis of a refrigeration system using nano fluid. *International Journal of Advanced Mechanical Engineering* 4(4): 459-470.
- [20] Cieśliński JT, Kaczmarczyk TZ. (2011). The effect of pressure on heat transfer during pool boiling of water-Al<sub>2</sub>O<sub>3</sub> and Water-Cu nanofluids on stainless steel smooth tube. *Chemical and Process Engineering* 32(4): 321-332. <https://doi.org/10.2478/v10176-011-0026-2>

## NOMENCLATURE

### Alphabetic

A	area	m <sup>2</sup>
cp	specific heat	W/(kg.K)
d <sub>i</sub>	test section inner diameter	m
h	heat transfer coefficient	W/(m <sup>2</sup> .K)
k	thermal conductivity	W/(m.K)
l	test section length	m
$\dot{m}$	mass flow rate	kg/s
Nu	Nusselt number	
Q	rate of heat transfer	W
$\dot{q}$	heat per unit surface area	W/m <sup>2</sup>
Re	Reynolds number	
T	temperature	K
V	volume	m <sup>3</sup>
z	mass fraction	%

### Subscripts

av	average.
c	condenser
e	evaporator
f	fluid, (R134a + oil)
i	inlet \ inner
np	Nano-Particles
nf	Nano-Fluid
o	outlet
P	nano-particle
s	surface
w	water



## Greek symbols

$\delta$	difference	
$\phi$	volume fraction	
$\mu$	dynamic viscosity	Pascal.s
$\rho$	density	kg/m <sup>3</sup>

## Abbreviations

C O P	coefficient of performance
LCD	liquid-crystal display
PID	proportional, integral and derivative
POE	polyester oil
TiO <sub>2</sub>	titanium dioxide

## APPENDICES

### Appendix A: Error analysis

To estimate the uncertainties of the *derived* quantities,  $\delta z$ ,  $\delta \phi$  and  $\delta h$ , etc, we first recall the uncertainties of the *participating* quantities, which are;

Length is measured using a vernier caliper with uncertainty  $\pm 0.02$  mm

Temperature: the resolution of the digital indicator is  $\pm 0.1$  °C.

The Nano-refrigerant *volume* flow rate,  $\dot{V}$ , is measured with an uncertainty of 0.05 L/min

Mass is weighed with the readability of 0.01 gm.

Then, we can estimate the uncertainties in the derived quantities as follows;

$$\delta z = \left( \frac{m_{np}}{m_{np} + m_f} \right) \sqrt{\left( \frac{\delta m_{np}}{m_{np}} \right)^2 + \left( \frac{\delta m_{np}^2 + \delta m_f^2}{(m_{np} + m_f)^2} \right)} \quad (A.1)$$

$$\delta \phi = \frac{z \rho_f}{\rho_{np} (1-z) + z \rho_f} \sqrt{\left( \frac{\rho_f \delta z}{\rho_f z} \right)^2 + \frac{(\rho_{np} \delta z)^2 + (\rho_f \delta z)^2}{(\rho_{np} (1-z) + z \rho_f)^2}} \quad (A.2)$$

$$\delta \rho_{nf} = \sqrt{(\delta \phi \rho_{np})^2 + (\delta \phi \rho_f)^2} \quad (A.3)$$

$$\delta m^* = (V \rho_{nf}^*) \sqrt{\left( \frac{\delta V^*}{V} \right)^2 + \left( \frac{\delta \rho_{nf}^*}{\rho_{nf}^*} \right)^2} \quad (A.4)$$

$$\delta Cp_{nf} = \frac{\phi \rho_{np} Cp_{np} + (1-\phi) \rho_f Cp_f}{\rho_{nf}} \sqrt{\frac{(\rho_{np} Cp_{np} \delta \phi)^2 + (\rho_f Cp_f \delta \phi)^2}{(\phi \rho_{np} Cp_{np} + (1-\phi) \rho_f Cp_f)^2} + \left( \frac{\delta \rho_{nf}}{\rho_{nf}} \right)^2} \quad (A.5)$$

$$\delta \mu_{nf} = \mu_f (1-\phi)^{2.5} \sqrt{\left( \frac{\delta \mu_f}{\mu_f} \right)^2 + 2.5 \left( \frac{\delta \phi}{(1-\phi)^{3.5}} \right)} \quad (A.6)$$

$$\delta k_{nf} = \sqrt{(k \rho_{np})^2 \left[ \left( \frac{\delta k_f}{k_f} \right)^2 + \left( \frac{\delta \rho_f}{\rho_f} \right)^2 \right] + [(1-\phi)k_f]^2 \left[ \left( \frac{\delta \phi}{\phi} \right)^2 + \left( \frac{\delta k_f}{k_f} \right)^2 \right]} \quad (A.7)$$

$$\delta Re = \frac{m d}{A \mu} \sqrt{\left( \frac{\delta m}{m} \right)^2 + 3 \left( \frac{\delta D}{D} \right)^2 + \left( \frac{\delta \mu}{\mu} \right)^2} \quad (A.8)$$

$$\delta h = \frac{[m Cp (T_o - T_i)]_{nf}}{\pi d_i L (T_{s,av} - T_{j,av})} \sqrt{\left( \frac{\delta m}{m} \right)^2 + \left( \frac{\delta Cp}{Cp} \right)^2 + \left( \frac{\delta T^2 + \delta T^2}{(T_o - T_i)^2} \right)^2 + \left( \frac{\delta d_i}{d_i} \right)^2 + \left( \frac{\delta L}{L} \right)^2 + \left( \frac{\delta T^2 + \delta T^2}{(T_{s,av} - T_{j,av})^2} \right)^2} \quad (A.9)$$

$$\delta Nu = \frac{h d}{k} \sqrt{\left( \frac{\delta h}{h} \right)^2 + \left( \frac{\delta d}{d} \right)^2 + \left( \frac{\delta k}{k} \right)^2} \quad (A.10)$$

$$\delta (C.O.P) = \frac{[Cp (T_o - T_i)]_{nf,e}}{[Cp (T_o - T_i)]_{nf,c}} \left[ \left( \frac{2 \delta Cp}{Cp} \right)_e^2 + \frac{4 \delta T^2}{(T_o - T_i)^2} \right] \quad (A.11)$$

According to the above formulas, the worst relative errors in the measured quantities are;

Relative error in measuring the weight raTiO<sub>2</sub> = 0.0017.

Relative error in measuring the volume fraction = 0.0016.

Relative error in measuring the nano-fluid density = 1.6 e-005.

Relative error in measuring the mass flow rate = 0.027.

Relative error in measuring the nano-fluid specific heat = 2.01 e-5.

Relative error in measuring the heat flux = 0.025.

Relative error in measuring the Nusselt number = 0.0123819.

Relative error in measuring the COP = 0.0294.

### Appendix B: Tests of the suggested Correlation

COEFFICIENTS OF EQUATION (15)			
	0.18	0.02	1.1 -0.36
Correlation	Experimental	Percentage	
512.60	505	1.5	
631.09	655	-3.6	
743.38	744	-0.08	
846.72	811	4.4	
539.22	522	3.3	
665.51	688	-3.2	
780.91	788	-0.8	
882.80	860	2.6	
549.02	545	0.7	
686.88	722	-4.8	
794.03	831	-4.4	
898.82	910	-1.2	
564.08	537	5.0	
693.70	708	-2.0	
813.17	811	0.2	
919.31	877	4.8	